This article was downloaded by: [Renmin University of China]
On: 13 October 2013, At: 10:27
Publisher: Taylor & Francis
Informa Ltd Registered in England and Wales Registered Number: 1072954 Registered office: Mortimer House, 37-41 Mortimer Street, London W1T 3JH, UK

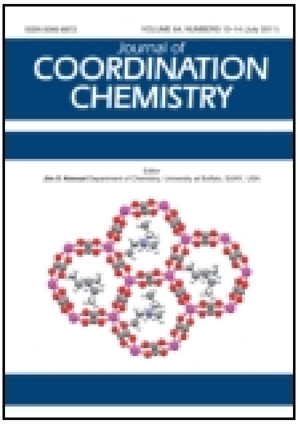

Journal of Coordination Chemistry
Publication details, including instructions for authors and subscription information:
http://www.tandfonline.com/loi/gcoo20

Synthesis and characterization of iridium polypyridyl complexes with ester groups with potential applications in covalent attachment to metal oxide surfaces

Joan Marie D. Zapiter [a] , Brian M. Tissue [a] & Karen J. Brewer [a]
[a] Department of Chemistry , Virginia Polytechnic Institute and State University , Blacksburg, Virginia 24061-0212, USA

Published online: 23 Sep 2011.

To cite this article: Joan Marie D. Zapiter , Brian M. Tissue & Karen J. Brewer (2011) Synthesis and characterization of iridium polypyridyl complexes with ester groups with potential applications in covalent attachment to metal oxide surfaces, Journal of Coordination Chemistry, 64:19, 3366-3375, DOI: 10.1080/00958972.2011.616928

To link to this article: http://dx.doi.org/10.1080/00958972.2011.616928

PLEASE SCROLL DOWN FOR ARTICLE

Taylor & Francis makes every effort to ensure the accuracy of all the information (the “Content”) contained in the publications on our platform. However, Taylor & Francis, our agents, and our licensors make no representations or warranties whatsoever as to the accuracy, completeness, or suitability for any purpose of the Content. Any opinions and views expressed in this publication are the opinions and views of the authors, and are not the views of or endorsed by Taylor & Francis. The accuracy of the Content should not be relied upon and should be independently verified with primary sources of information. Taylor and Francis shall not be liable for any losses, actions, claims, proceedings, demands, costs, expenses, damages, and other liabilities whatsoever or howsoever caused arising directly or indirectly in connection with, in relation to or arising out of the use of the Content.

This article may be used for research, teaching, and private study purposes. Any substantial or systematic reproduction, redistribution, reselling, loan, sub-licensing, systematic supply, or distribution in any form to anyone is expressly forbidden. Terms &

Journal of Coordination Chemistry
Vol. 64, No. 19, 10 October 2011, 3366–3375

Synthesis and characterization of iridium polypyridyl complexes with ester groups with potential applications in covalent attachment to metal oxide surfaces

JOAN MARIE D. ZAPITER, BRIAN M. TISSUE* and KAREN J. BREWER*

Department of Chemistry, Virginia Polytechnic Institute and State University,
Blacksburg, Virginia 24061–0212, USA

(*Received 22 April 2011; in final form 4 August 2011*)

We report the synthesis and characterization of two iridium polypyridyl complexes, $[Ir(deeb)_2Cl_2](PF_6)$ and $[Ir(deeb)_2(dpp)](PF_6)_3$, where deeb = diethyl-2,2′-bipyridine-4,4′-dicarboxylate and dpp = 2,3-bis(2-pyridyl)pyrazine. From ^{1}H NMR spectral data, the two deeb ligands are attached to Ir *cis* to each other. Mass spectra contain fragmentation patterns of the $(M\text{-}PF_6)^+$ and $(M\text{-}3PF_6)^{3+}$ molecular ions for $[Ir(deeb)_2Cl_2](PF_6)$ and $[Ir(deeb)_2(dpp)](PF_6)_3$, respectively. The electronic absorption spectrum of $[Ir(deeb)_2Cl_2](PF_6)$ shows maxima at 308 nm and 402 nm, which are assigned as $^1\pi \rightarrow \pi^*$ and metal-to-ligand charge transfer transitions, respectively. $[Ir(deeb)_2(dpp)](PF_6)_3$ exhibits peaks due to $^1\pi \rightarrow \pi^*$ transitions at 322 nm and 334 nm. $[Ir(deeb)_2Cl_2](PF_6)$ has emission peaks at 538 nm in acetonitrile and 567 nm in the solid state, with lifetimes of 1.71 µs and 0.35 µs, respectively. $[Ir(deeb)_2Cl_2](PF_6)$ has an unusually higher quantum yield than analogous compounds. $[Ir(deeb)_2(dpp)](PF_6)_3$ has emission peaks at 540 nm in acetonitrile and 599 nm in the solid state with lifetimes of 1.23 µs and 0.14 µs, respectively. Cyclic voltammetry of $[Ir(deeb)_2Cl_2](PF_6)$ yields two reversible couples at −0.72 and −0.87 V *versus* Ag/AgCl, both corresponding to deeb ligand reductions, and a quasi-reversible couple at −1.48 V corresponding to $Ir^{3+/+}$ reduction. Electrochemical reduction of $[Ir(deeb)_2(dpp)](PF_6)_3$ yields couples at −0.38, −0.54, −0.71, and −1.33 V, assigned as $deeb^{0/-}$, $deeb^{0/-}$, $dpp^{0/-}$, and $Ir^{3+/+}$ reductions, respectively.

Keywords: deeb; Bipyridine; Photochemistry

1. Introduction

Transition metal complexes containing polypyridyl ligands such as 2,2′-bipyridine (bpy) have been studied extensively due to their ability to absorb light and form excited states that are applicable to photovoltaics and photocatalysis. Transition metal complexes have several advantages in photochemical reactions [1, 2]. They have large molar absorption coefficients and quantum yields throughout the UV and visible spectral regions and their photophysical and chemical properties can be tuned by changing the metal center or altering the ligands [3, 4].

Iridium complexes are excellent light absorbers and were reported as energy donors to improve emissive materials, such as systems containing lanthanide ions [5–10].

---

*Corresponding authors. Email: tissue@vt.edu; kbrewer@vt.edu

Journal of Coordination Chemistry
ISSN 0095-8972 print/ISSN 1029-0389 online © 2011 Taylor & Francis
http://dx.doi.org/10.1080/00958972.2011.616928

Eu^{3+} in ionic solids is used in fluorescent lighting, lasers, displays, and analytical assays. Eu^{3+} luminescence is usually excited by energy transfer from a sensitizer due to the weak oscillator strength of 4f–4f transitions [11, 12]. One example uses iridium fluorinated polypyridyl complexes connected to a Eu^{3+} chelate *via* carboxylate groups [9]. The iridium monometallic unit has $^1\pi \rightarrow \pi^*$ transitions in the UV region and emits blue light with maxima at 460 and 490 nm. The terpyridine-capped europium unit has strong red emission at 615 nm. Exciting the iridium complex at 400 nm produces white light emission due to the combination of the blue and red emission from the iridium and europium moieties, respectively. Similar systems that use phen (1,10-phenanthroline) [6, 7], non-fluorinated ppy (2-phenylpyridine), and π-extended bridging ligands [5] on the Ir unit have also been reported to undergo energy transfer to a europium chelate.

Metal complexes can be attached on the surface of lanthanide oxides *via* ligands with carboxylate ester groups such as deeb (4,4′-$(COOCH_2CH_3)_2$-bpy), which is a similar method used in dye-sensitized solar cells [13–19]. In deeb, the ester is known to be hydrolyzed into its carboxylate form in solution and in the presence of surface hydroxyl groups on the metal oxide nanoparticle [13–19]. Using deeb instead of its carboxylic acid analog reduces complications in the synthesis, as pH will not affect isolating the ligand and its complexes [19]. The ester group also serves as a spectroscopic probe to determine the structure. In this work, iridium complexes containing deeb were prepared to coat europium oxide nanoparticles for future studies of the photophysical processes between iridium and europium. In spite of difficulties in synthesis [4], iridium complexes are chosen due to their green emissive states whose energies lie above the Eu^{3+} $^5D_0$ state. Additionally, one of the internal ligand (IL) states of these complexes is also slightly higher in energy compared to the Eu–O charge transfer band of europium oxide. Due to the very close energies, it is likely that the iridium complexes transfer energy to europium. $[Ir(deeb)_2Cl_2](PF_6)$ serves as a starting point for synthetic and photophysical experiments. $[Ir(deeb)_2(dpp)](PF_6)_3$ was synthesized because the chloride ligands in the first complex are expected to be labile enough to allow the iridium center to coordinate with oxygen on the metal oxide surface. Replacing chlorides with dpp will allow a more uniform mode of attachment of the complexes on the oxide surface as well as a lower energy excited state that is closer to the Eu^{3+} $^5D_0$ state.

2. Experimental

2.1. *Molecular synthesis*

Iridium(III) chloride hydrate (Alfa Aesar, Premion 99.99%), 2,2′-bipyridine-4,4′-dicarboxylic acid (Strem), potassium hexafluorophosphate (KPF_6, Fluka), spectral grade acetonitrile (Burdick and Jackson), HPLC-grade solvents, dichloromethane (Fisher), diethyl ether (Fisher), ethyl acetate (Fisher), methanol (Fisher), and ethanol (AAPER) were used as received. The ligand deeb was prepared as reported previously [20].

2.1.1. *cis*-Dichlorobis(diethyl-2,2′-bipyridine-4,4′-dicarboxylate)iridium(III) hexafluorophosphate, $[Ir(deeb)_2Cl_2](PF_6)$. The synthetic procedure for the iridium dichloride complex was patterned after its rhodium analog [21]. It was prepared by reacting 0.64 g

(1.8 mmol) of $IrCl_3 \cdot \times H_2O$ and 1.41 g (4.7 mmol) of deeb in 230 mL of 2 : 1 ethanol : H_2O, previously deoxygenated with argon for at least 15 min. The mixture was heated at reflux for 66 h, filtered hot, and the ethanol was evaporated from the filtrate. The filtrate was then diluted with 10 mL H_2O and 30 mL of a saturated aqueous KPF_6 solution was added dropwise. The resulting precipitate was filtered, washed with cold water and diethyl ether, and dried in vacuum. The solid was then dissolved in small amounts of acetone and flash precipitated in diethyl ether. It was purified by recrystallizing twice in hot 4 : 1 methanol : ethyl acetate to isolate a bright yellow solid. Typical yield is ≈33% (0.60 g, 0.59 mmol). ^1H NMR (400 MHz, $(CD_3)_2CO$): δ (ppm) 10.08 (d, 2 H, $J = 6$ Hz), 9.45 (s, 2 H), 9.34 (s, 2 H), 8.62 (d, 2 H, $J = 6$ Hz), 8.36 (d, 2 H, $J = 6$ Hz), 7.90 (d, 2 H, $J = 6$ Hz), 4.60 (q, 4 H, $J_1 = J_2 = J_3 = 7$ Hz), 4.44 (q, 4 H, $J_1 = J_2 = J_3 = 7$ Hz), 1.49 (t, 6 H, $J_1 = J_2 = 7$ Hz), 1.35 (t, 6 H, $J_1 = J_2 = 7$ Hz). ESI-MS (*m*/*z*): 863 found and Calcd $[M\text{-}PF_6]^+$.

2.1.2. Bis(diethyl-2,2′-bipyridine-4,4′-dicarboxylate)-2,3-bis(2-pyridyl)pyrazineiridium(III) hexafluorophosphate, $[Ir(deeb)_2(dpp)](PF_6)_3$. The complex was prepared by reacting $[Ir(deeb)_2Cl_2](PF_6)$ (0.11 g, 0.1 mmol) with 20 times excess of both dpp (0.49 g, 2 mmol) and $TlPF_6$ (0.76 g, 2 mmol) in 5 mL CH_3CN. The mixture was heated to reflux for 18 h and cooled to room temperature. The mixture was filtered and the solvent from the filtrate was removed by evaporation. Water, 50 mL, was added, after which 10 mL of saturated aqueous KPF_6 was added dropwise. The off-white to light tan solids were recovered by vacuum filtration and purified by elution through a Sephadex LH-20 (hydroxypropylated cross-linked dextran) column with 3 : 1 CH_3CN : ethanol as mobile phase. The first fraction was collected, the solvent evaporated, and the solids flash precipitated in diethyl ether using minimal amounts of acetonitrile. Yield was ≈20% (0.29 g, 0.20 mmol). ^1H NMR (400 MHz, $(CD_3)_2CO$): δ (ppm) 9.57 (s, 1 H), 9.54 (s, 3 H), 8.90 (d, 1 H, $J = 3$ Hz), 8.79 (d, 1 H, $J = 6$ Hz), 8.71 (d, 1 H, $J = 4$ Hz), 8.61 (d, 1 H, $J = 6$ Hz), 8.55 (d, 1 H, $J = 6$ Hz), 8.51 (d, 1 H, $J = 7$ Hz), 8.48 (d, 1 H, $J = 6$ Hz), 8.43 (d, 1 H, $J = 3$ Hz), 8.33 (d, 1 H, $J = 5$ Hz), 8.19 (m, 6 H), 7.72 (m, 1 H), 7.67 (d, 1 H, $J = 9$ Hz), 4.49 (m, 8 H), 1.37 (m, 12 H). ESI-MS (*m*/*z*): 342 found and Calcd $[M\text{-}3PF_6]^{3+}$.

2.2. *Spectroscopy*

^1H NMR spectra were recorded at room temperature using a 400 MHz spectrometer (Varian Inova). Sample solutions of the metal complexes were prepared by dissolving ≈20 mg of solid in 0.5 mL of deuterated solvent that were sonicated and syringe-filtered prior to analysis. Electro-spray ionization mass spectra were obtained using an LC-ESI-TOF spectrometer (Agilent) at room temperature. Calculated mass spectra were obtained from the Scientific Instrument Services website (Sisweb.com). Electronic absorption spectra in solution were recorded at room temperature using a diode-array spectrophotometer (Hewlett-Packard 8452 A) with a 2-nm resolution. All measurements used Burdick and Jackson UV-grade acetonitrile as solvent in 1-cm quartz cuvettes.

Emission spectra were recorded from solid and solution samples at room temperature using a spectrofluorometer (Photon Technologies International QM-40). The system contains a high intensity continuous xenon excitation source and a red-sensitive photomultiplier tube operating in photon counting mode. Emission is collected in a 90° geometry with 4-nm resolution. For solid measurements, samples were packed into a 3-mm diameter and 2-mm deep depression in a black fiberglass block. Measurements of solutions were carried out in 1-cm path length cuvettes. Emission spectra were corrected for PMT response and normalized.

Lifetimes were measured using a pulsed nitrogen laser at 337 nm (Photon Technologies International). The laser beam was focused at 90° and 45° angles to solution and solid samples, respectively, using a 60-mm focal length lens. Sample preparation is the same as used for emission measurements. Emission was collected through a 75-mm lens, focused through a cut-off or bandpass filter onto a photomultiplier tube (Photon Technologies International R928) and recorded by averaging 300 or more laser pulses using a 300 MHz oscilloscope (LeCroy 9361). All lifetime values were approximated by exponential curve fitting using Origin (OriginLab Corp.) after subtracting a background signal due to laser scatter from the sample holder.

2.3. *Electrochemistry*

Cyclic voltammograms were recorded using a potentiostat (Bioanalytical Systems) with a platinum wire auxiliary electrode, a 1.9-mm diameter glassy carbon disc working electrode and a Ag/AgCl reference electrode (0.29 V *vs.* NHE) in one-compartment cells. Metal complex solutions were prepared using 0.1 mol L^{-1} tetrabutylammonium hexafluorophosphate (TBAH) in UV-grade acetonitrile (Burdick and Jackson) as supporting electrolyte.

3. Results and discussion

Figure 1 shows ^1H NMR spectra for the newly prepared $[Ir(deeb)_2Cl_2](PF_6)$. Chemical shift assignments for solvent and residual water were based on published values [22]. The presence of methyl protons at 1.49 ppm (t, 6 H) and 1.35 ppm (t, 6 H), and methylene protons at 4.60 ppm (q, 4 H) and 4.44 ppm (q, 4 H) in $[Ir(deeb)_2Cl_2](PF_6)$ indicate retention of the ester moieties of deeb upon formation of the complex. ^1H-^1H COSY NMR spectrum of the complex at the aromatic region is shown in figure 1(c). The chemical shift at 8.62 ppm is assigned to the proton in the 5 position of the bipyridine unit because of its correlation with the most downfield proton in the 6 position. The peaks at 7.90 and 8.36 ppm are assigned to the 5′ and 6′ protons because of their correlation with each other as seen in the ^1H-^1H COSY spectrum. These assignments are made to correct previous assignments for the ruthenium and rhodium analogs [21, 23]. The 1-D and 2-D spectra show multiplets and integration that are consistent with those reported for $[Ir(bpy)_2Cl_2](PF_6)$ sans the 4 and 4′ protons [24]. The ESI–MS spectrum in figure 2(a) is consistent with the $(M\text{-}PF_6)^+$ ion (863, found and Calcd).

The ^1H NMR spectrum and assignments of $[Ir(deeb)_2(dpp)](PF_6)_3$, which are consistent with those of $[Ru(deeb)_2(dpp)](PF_6)_3$ [25], are also shown in figure 1. The

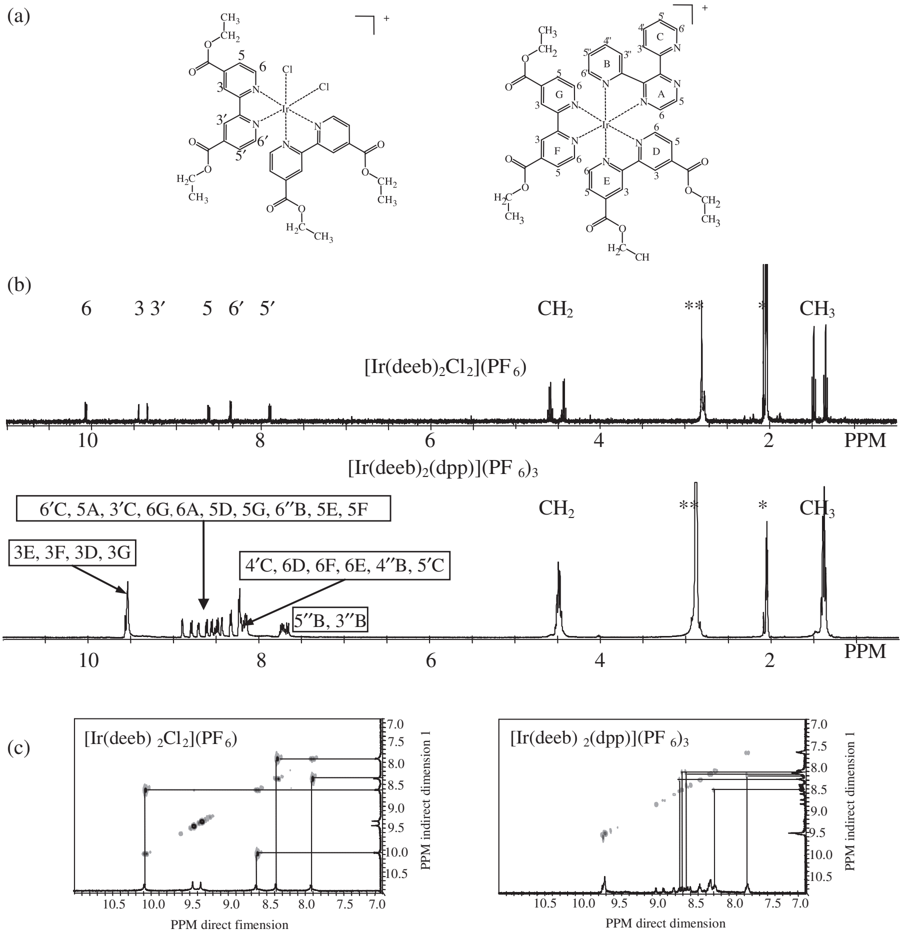

Figure 1. (a) Structures and chemical shift assignments, (b) 1D ^{1}H NMR spectra, and (c) ^{1}H-^{1}H COSY NMR spectra of aromatic regions of [Ir(deeb)$_2$Cl$_2$](PF$_6$) and [Ir(deeb)$_2$(dpp)](PF$_6$)$_3$ in (CD$_3$)$_2$CO, where deeb = diethyl-2,2′-bipyridine-4,4′-dicarboxylate, dpp = 2,3-bis(2-pyridyl)pyrazine (* and ** indicate solvent and water, respectively).

ESI–MS spectrum in figure 2(b) displays a fragmentation pattern for (M-3PF$_6$)$^{3+}$ (342, found and Calcd).

The electronic absorption spectrum of [Ir(deeb)$_2$Cl$_2$](PF$_6$) (figure 3a) displays a deeb transition at 308 nm and a small peak at 402 nm assigned to a ^{1}MLCT, Ir(dπ) → deeb(π*), transition. Table 1 compares the spectral properties of [Ir(deeb)$_2$Cl$_2$](PF$_6$) with its bpy analog [26]. The absorption maxima are slightly red-shifted due to electron-withdrawing effect of the ester group, which lowers the deeb π* orbital. Excited iridium complexes form metal-to-ligand charge transfer (MLCT) or IL emissive excited states, depending on the electron density around the metal. If the ligands are anionic, in the case of halide or cyclometallating ligands, the emissive state tends to be an MLCT state because there is sufficient charge density on the metal; otherwise, emission is due to an IL excited state [4, 27]. [Ir(bpy)$_2$Cl$_2$](PF$_6$), for instance, has an emissive ^{3}MLCT state at 510 nm [26]. Emission spectra of [Ir(deeb)$_2$Cl$_2$](PF$_6$) in

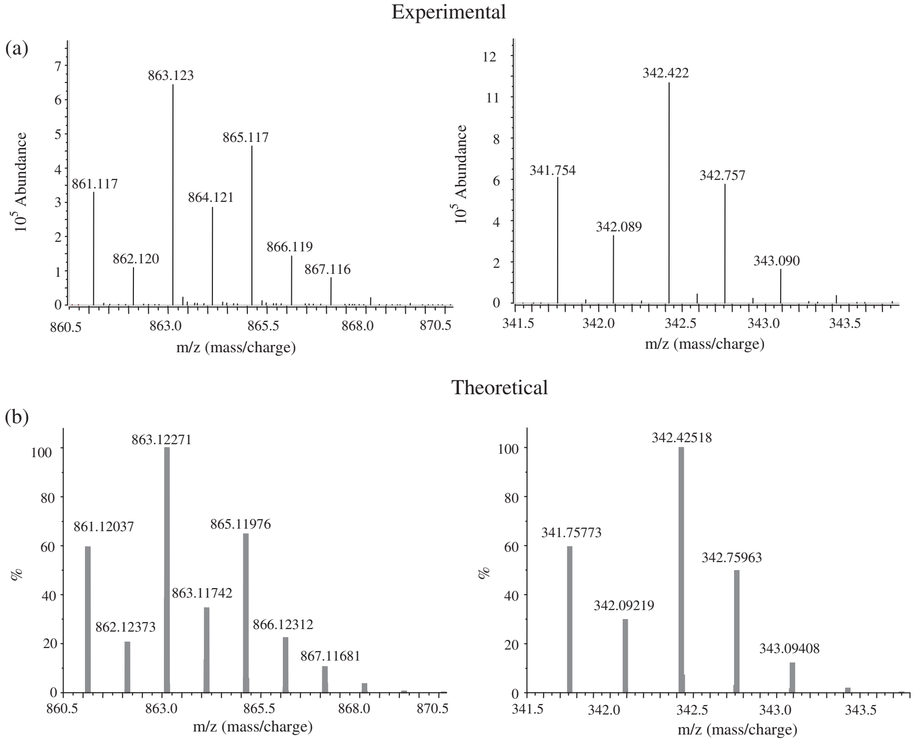

Figure 2. Experimental and theoretical mass spectral data for (a) $[Ir(deeb)_2Cl_2](PF_6)$ and (b) $[Ir(deeb)_2(dpp)](PF_6)_3$, where deeb = diethyl-2,2′-bipyridine-4,4′-dicarboxylate, dpp = 2,3-bis(2-pyridyl) pyrazine.

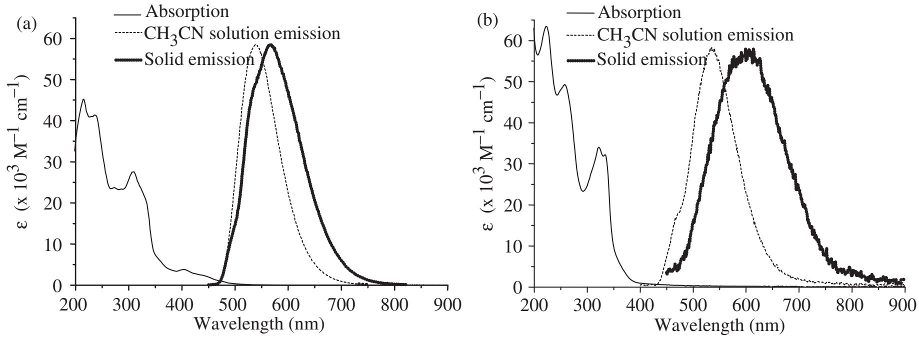

Figure 3. Electronic absorption and normalized emission spectra at room temperature of (a) $[Ir(deeb)_2Cl_2](PF_6)$ and (b) $[Ir(deeb)_2(dpp)](PF_6)_3$ in CH_3CN and as solid (deeb = diethyl-2,2′-bipyridine-4,4′-dicarboxylate, dpp = 2,3-bis(2-pyridyl)pyrazine).

figure 3(a) reveal a broad peak with a maximum at 538 nm and a tail that extends beyond 700 nm. The complex in powder form shows a similar spectrum that is red-shifted with a peak at 567 nm. Other iridium complexes used for organic light-emitting diodes (OLEDs) and light-emitting electrochemical cells (LECs) show similar

Table 1. Electronic spectral data for [Ir(deeb)$_2$Cl$_2$](PF$_6$), [Ir(bpy)$_2$Cl$_2$]$^+$ [26, 31, 32], and [Ir(deeb)$_2$(dpp)](PF$_6$)$_3$ at room temperature.

	Absorption		Emission			
Complex	λ_{max} (nm)	ε ($\times 10^{-3}$ L mol^{-1}cm^{-1})		λ_{max} (nm)	τ (µs)	Φ
[Ir(deeb)$_2$Cl$_2$](PF$_6$)	308	28	CH$_3$CN	538	1.71 ± 0.17	0.33
	402	3.7	Solid	567	0.35 ± 0.02	–
	442 (sh)	2.2				
[Ir(bpy)$_2$Cl$_2$]$^+$	290	27	CH$_3$CN	510	0.344 ± 0.010	0.0066
	385	2.8	DMF	547	0.335 ± 0.015	0.0098
	430 (sh)	1.1				
[Ir(deeb)$_2$(dpp)](PF$_6$)$_3$	322	34	CH$_3$CN	540	1.23 ± 0.03	0.013
	334	32	Solid	599	0.14 ± 0.02	–

shifts [28, 29]. As shown in figure 4(a), the room temperature excited-state lifetime of [Ir(deeb)$_2$Cl$_2$](PF$_6$) in acetonitrile is 1.71 ± 0.17 µs, which is longer compared to those of similar compounds in DMF at room temperature: [Ir(bpy)$_2$Cl$_2$]$^+$, 0.333 µs; [Ir(phen)$_2$Cl$_2$]$^+$, 0.324 µs; and [Ir(5,6-Mephen)$_2$Cl$_2$]$^+$, 0.840 µs [30, 31]. A high quantum yield of emission for [Ir(deeb)$_2$Cl$_2$](PF$_6$) ($\Phi = 0.33$) was also observed. For [Ir(bpy)$_2$Cl$_2$]$^+$, the quantum yield is 0.0066 in acetonitrile at room temperature [32]. Both a lower non-radiative rate and a higher radiative rate for [Ir(deeb)$_2$Cl$_2$](PF$_6$) compared to the other compounds lead to a higher quantum yield. The lifetime for the solid at room temperature displays a single exponential decay profile giving $\tau = 0.35 \pm 0.02$ µs. Reduction in the lifetime in the solid state may be attributed to concentration quenching or energy transfer to quenching defects.

Figure 3(b) shows the electronic absorption and emission spectra of [Ir(deeb)$_2$(dpp)](PF$_6$)$_3$. The absorption spectrum contains peaks in the UV region that are similar to those in the spectrum of [Ir(bpy)$_3$]$^{3+}$ which were assigned as $^1\pi \rightarrow \pi^*$ transitions from the ligands [33]. The emission spectrum at room temperature contains a broad band centered at 540 nm, which is red shifted to 599 nm in the solid state. Luminescence is assigned to relaxation of the $^3\pi \rightarrow \pi^*$ excited state, as in [Ir(bpy)$_3$]$^{3+}$ [33]. The assignment of the emissive state of [Ir(deeb)$_2$(dpp)](PF$_6$)$_3$ was patterned after [Ir(bpy)$_3$]$^{3+}$ and other tris-chelated iridium compounds which were primarily $^3\pi \rightarrow \pi^*$ with some ^{3}MLCT character according to the work of Demas *et al.* [33, 34] and those included in the review of Flamigni *et al.* [4]. The electron-donating chlorides destabilize the Ir orbitals providing for MLCT of the lowest lying state. The decay curve of [Ir(deeb)$_2$(dpp)](PF$_6$)$_3$ is shown in figure 4(b) and the lifetime was found to be 1.23 ± 0.03 µs and 0.14 ± 0.02 µs in acetonitrile solution and in the solid state, respectively, which is comparable to that of [Ir(bpy)$_3$]$^{3+}$ (2.4 µs in methanol [34]) at room temperature.

Table 2 and figure 5 give electrochemical data for [Ir(deeb)$_2$Cl$_2$](PF$_6$) with those for analogous compounds [Ir(bpy)$_2$Cl$_2$](PF$_6$) and [Ir(dpp)$_2$Cl$_2$](PF$_6$) previously reported by our group [26]. Two reversible reductive couples at −0.72 V and −0.87 V, assigned to deeb reductions, followed by a two-electron, quasi-reversible iridium reduction at −1.48 V were observed for [Ir(deeb)$_2$Cl$_2$](PF$_6$), consistent with previous reports on the bpy and dpp analogs. The shoulder at −1.07 V may be attributed to reduction of a

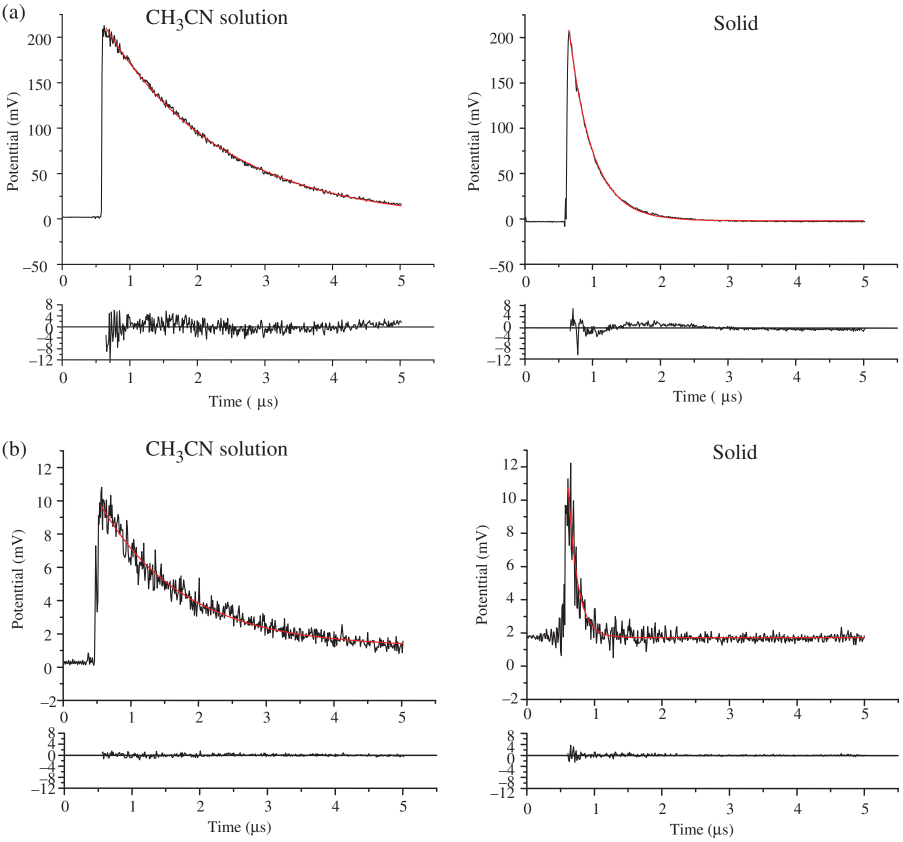

Figure 4. Lifetime decay curves and residual plots of (a) $[Ir(deeb)_2Cl_2](PF_6)$ and (b) $[Ir(deeb)_2(dpp)](PF_6)_3$ in CH_3CN and as solid at room temperature (deeb = diethyl-2,2′-bipyridine-4,4′-dicarboxylate, dpp = 2,3-bis(2-pyridyl)pyrazine).

Table 2. Electrochemical data for $[Ir(deeb)_2Cl_2](PF_6)$, $[Ir(bpy)_2Cl_2](PF_6)$ [26], $[Ir(dpp)_2Cl_2](PF_6)$ [26], and $[Ir(deeb)_2(dpp)](PF_6)_3$ using 0.1 mol L^{-1} TBAH in CH_3CN as supporting electrolyte at room temperature.

Complex	E_p^a (V)	E_p^a (V)	$E_{1/2}$ (V)	Assignment
$[Ir(deeb)_2Cl_2](PF_6)$	−0.67	−0.78	−0.72	deeb$^{0/-}$
	−0.87	−0.93	−0.87	deeb$^{0/-}$
		−1.48		Ir$^{3+/+}$
$[Ir(bpy)_2Cl_2](PF_6)$	−1.10	−1.25	−1.18	bpy$^{0/-}$
	−1.30	−1.47	−1.39	bpy$^{0/-}$
		−2.12		Ir$^{3+/+}$
$[Ir(dpp)_2Cl_2](PF_6)$	−0.80	−0.86	−0.83	dpp$^{0/-}$
	−1.03	−1.09	−1.06	dpp$^{0/-}$
		−1.79		Ir$^{3+/+}$
$[Ir(deeb)_2(dpp)](PF_6)_3$	−0.34	−0.42	−0.38	deeb$^{0/-}$
	−0.49	−0.58	−0.54	deeb$^{0/-}$
	−0.67	−0.76	−0.71	dpp$^{0/-}$
		−1.33		Ir$^{3+/+}$

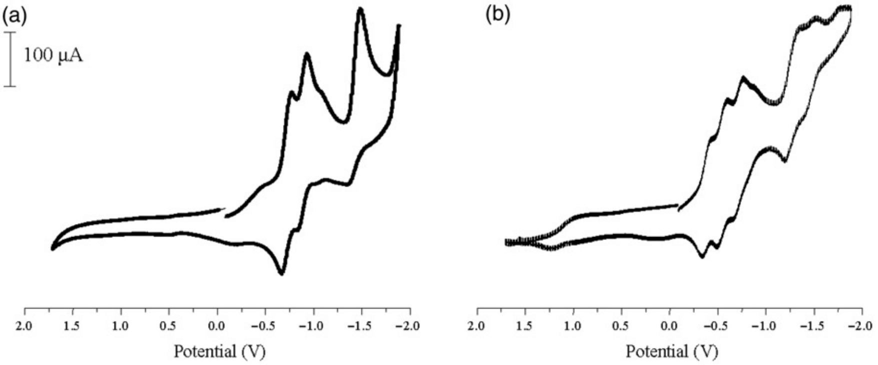

Figure 5. Cyclic voltammograms of (a) $[Ir(deeb)_2Cl_2](PF_6)$ and (b) $[Ir(deeb)_2(dpp)](PF_6)_3$ using 0.1 mol L^{-1} TBAH in CH_3CN as supporting electrolyte at room temperature (deeb = diethyl-2,2′-bipyridine-4,4′-dicarboxylate, dpp = 2,3-bis(2-pyridyl)pyrazine).

$[Ir(deeb)_2Cl]^+$ species, which could have formed from reducing the starting material and could clearly be defined at lower scan rates [35].

Less negative reduction values for deeb compared to bpy and dpp as seen in the electrochemical data for the dichloride complexes imply that deeb is easier to reduce than the other two ligands. Hence, the first three reductions for $[Ir(deeb)_2(dpp)](PF_6)_3$ at −0.38 V, −0.54 V and −0.71 V are assigned to be $deeb^{0/-}$, $deeb^{0/-}$ and $dpp^{0/-}$ reductions, respectively. Differences in the deeb reduction potentials for $[Ir(deeb)_2Cl_2](PF_6)$ and $[Ir(deeb)_2(dpp)](PF_6)_3$ could be due to the differences in the nature of their excited states which modulate their abilities for electron transfer. In addition, the chlorides in $[Ir(deeb)_2Cl_2](PF_6)$ are strongly electron-donating, destabilizing the iridium orbitals making it easier to be reduced in $[Ir(deeb)_2Cl_2](PF_6)$. A shoulder similar to that in $[Ir(deeb)_2Cl_2](PF_6)$ occurs at −0.78 V, which could be attributed to part of the deeb ligand detaching from the metal to form a $[Ir(deeb)_2(dpp)]^{2+}$ species. Another shoulder at −1.49 V appears for $[Ir(deeb)_2(dpp)](PF_6)_3$, a reductive couple similarly observed for trischelated iridium complexes like $[Ir(bpy)_3]^{3+}$ and could be assigned as reduction of a $[Ir(deeb)_2(dpp)]^{1-}$ species [35].

4. Conclusion

$[Ir(deeb)_2Cl_2](PF_6)$ and $[Ir(deeb)_2(dpp)](PF_6)_3$ were synthesized and characterized. ^1H NMR data were consistent with previously reported rhodium and ruthenium analogs with assignments confirmed by ^1H-^1H COSY spectroscopy. Electronic absorption spectra of both complexes show ligand $^1\pi \rightarrow \pi^*$ and ^{1}MLCT transitions in the UV and visible regions. Emission spectra of $[Ir(deeb)_2Cl_2](PF_6)$ and $[Ir(deeb)_2(dpp)](PF_6)_3$ in solution and as solids show green emission from the ^{3}MLCT and $^3\pi \rightarrow \pi^*$ states, respectively. $[Ir(deeb)_2Cl_2](PF_6)$ has a quantum yield that is unusually higher than those of similar bipyridyl compounds. The microsecond lifetimes make them suitable as energy transfer donors to suitable acceptors and as components for OLEDs and LECs.

The ester linkages on deeb provide for covalent coupling to metal oxide surfaces to investigate the properties of these systems on surfaces.

Acknowledgments

We would like to thank Mr William Bebout of the Analytical Services Laboratory, Department of Chemistry at Virginia Tech for the mass spectral data and Mr Rongwei Zhou for his help in preparing the solid emission sample holders. We are also grateful to the Chemical Sciences, Geosciences and Biosciences Division, Office of Basic Energy Sciences, Office of Sciences, US Department of Energy DE FG02-05ER15751 for partial support of this work.

References

[1] J.H. Alstrum-Acevedo, M.K. Brennaman, T.J. Meyer. *Inorg. Chem.*, **44**, 6802 (2005).
[2] V. Balzani, G. Bergamini, P. Ceroni. *Coord. Chem. Rev.*, **252**, 2456 (2008).
[3] V. Balzani, A. Juris, M. Venturi, S. Campagna, S. Serroni. *Chem. Rev.*, **96**, 759 (1996).
[4] L. Flamigni, A. Barbieri, C. Sabatini, B. Ventura, F. Barigelletti. *Top. Curr. Chem.*, **281**, 143 (2007).
[5] N.M. Tart, D. Sykes, I. Sazanovich, I.S. Tidmarsh, M.D. Ward. *Photochem. Photobiol. Sci.*, **9**, 886 (2010).
[6] F.F. Chen, Z.Q. Bian, Z.W. Liu, D.B. Nie, Z.Q. Chen, C.H. Huang. *Inorg. Chem.*, **47**, 2507 (2008).
[7] F.F. Chen, Z.Q. Bian, B. Lou, E. Ma, Z.W. Liu, D.B. Nie, Z.Q. Chen, J. Bian, Z.N. Chen, C.H. Huang. *Dalton Trans.*, 5577 (2008).
[8] Z.Q. Chen, Z.Q. Bian, C.H. Huang. *Adv. Mater.*, **22**, 1534 (2010).
[9] P. Coppo, M. Duati, V.N. Kozhevnikov, J.W. Hofstraat, L. De Cola. *Angew. Chem. Int. Ed.*, **44**, 1806 (2005).
[10] M. Mehlstaeubl, G.S. Kottas, S. Colella, L. De Cola. *Dalton Trans.*, 2385 (2008).
[11] J.-C.G. Bunzli, C. Piguet. *Chem. Soc. Rev.*, **34**, 1048 (2005).
[12] W.M. Yen, S. Shionoya, H. Yamamoto. *Phosphor Handbook*, pp. 192–199, CRC Press/Taylor and Francis, Boca Raton, FL (2007).
[13] G.T. Higgins, B.V. Bergeron, G.M. Hasselmann, F. Farzad, G.J. Meyer. *J. Phys. Chem.*, **110**, 2598 (2006).
[14] G.J. Meyer. *Inorg. Chem.*, **44**, 6852 (2005).
[15] G.J. Meyer. *J. Photochem. Photobiol.*, **158**, 119 (2003).
[16] P. Qu, G.J. Meyer. *Langmuir*, **17**, 6720 (2001).
[17] P. Qu, D.W. Thompson, G.J. Meyer. *Langmuir*, **16**, 4662 (2000).
[18] C.A. Kelly, F. Farzad, D.W. Thompson, J.M. Stipkala, G.J. Meyer. *Langmuir*, **15**, 7047 (1999).
[19] C.A. Kelly, F. Farzad, D.W. Thompson, G.J. Meyer. *Langmuir*, **15**, 731 (1999).
[20] G. Wolfbauer, A.M. Bond, D.R. MacFarlane. *Inorg. Chem.*, **38**, 3836 (1999).
[21] J.M.D. Zapiter, B.M. Tissue, K.J. Brewer. *Inorg. Chem. Commun.*, **11**, 51 (2008).
[22] H.E. Gottlieb, V. Kotlyar, A. Nudelman. *J. Org. Chem.*, **62**, 7512 (1997).
[23] R. Hermann, M. Graetzel, H.U. Nissen, V. Shklover, M.K. Nazeeruddin, S.M. Zakeeruddin, C. Barbe, A. Kay, T. Haibach, W. Steurer. *Chem. Mater.*, **9**, 430 (1997).
[24] R.E. DeSimone, R.S. Drago. *Inorg. Chem.*, **8**, 2517 (1969).
[25] B.V. Bergeron, G.J. Meyer. *J. Phys. Chem.*, **107**, 245 (2003).
[26] S.C. Rasmussen, M.M. Richter, E. Yi, H. Place, K.J. Brewer. *Inorg. Chem.*, **29**, 3926 (1990).
[27] I.M. Dixon, J.P. Collin, J.P. Sauvage, L. Flamigni, S. Encinas, F. Barigelletti. *Chem. Soc. Rev.*, **29**, 385 (2000).
[28] W. He, D.-J. Zu, D.-M. Liu, R. Cheng. *Inorg. Chim. Acta*, **365**, 78 (2011).
[29] A.M. Talarico, I. Aiello, A. Bellusci, A. Crispini, M. Ghedini, N. Godbert, T. Pugliese, E. Szerb. *Dalton Trans.*, **39**, 1709 (2010).
[30] R.J. Watts, D. Missimer. *J. Am. Chem. Soc.*, **100**, 5350 (1978).
[31] R.J. Watts, S. Efrima, H. Metiu. *J. Am. Chem. Soc.*, **101**, 2742 (1979).
[32] B. Divisia, P.C. Ford, R.J. Watts. *J. Am. Chem. Soc.*, **102**, 7264 (1980).